

# AN ELASTIC BEARING FOR RECTILINEAR TRANSLATIONS AND ITS APPLICATION WITHIN A MICRO METROLOGY INSTRUMENT

Mathieu Barraja<sup>1</sup>, R. Ryan Vallance<sup>1</sup>, George Mathai<sup>1</sup> and Eric R. Marsh<sup>2</sup>

<sup>1</sup>Precision Systems Laboratory, The George Washington University  
Washington, D.C. USA

<sup>2</sup>Machine Dynamics Research Laboratory, The Pennsylvania State University  
University Park, PA USA

## INTRODUCTION

This paper describes an elastic bearing used for independent rectilinear displacements in two orthogonal directions. The topology of the bearing, illustrated in Fig. 1, uses an arrangement of beams and masses. This topology is suited to high precision applications that require small displacements such as in scanning probe microscopy [1], and we are using the bearing in a new instrument for measuring roundness profiles of micro scale components [2, 3].

The bearing consists of a rigid frame, four intermediate masses  $m$  and a center mass  $M$ , as shown in Fig. 1. The frame and the center mass are connected to the intermediate masses by twenty-four beams. Each beam has fixed-guided boundary conditions (no displacement or rotation at one end and no rotation at the opposite end). Twelve beams are parallel to the  $x$  axis, and twelve are parallel to the  $y$  axis. Displacement of the center mass with respect to the rigid frame is produced by applying a normal force on an intermediate mass. The beams that are orthogonal to the direction of the applied load bend, while the beams that are parallel to the direction of the applied load are compressed or extended. The dimensions of all the beams are selected to provide compliance under bending while remaining stiff under axial loading.

This bearing topology provides a planar arrangement for rectilinear motion with some significant benefits for precision engineering. First, rectilinear motion is achieved without having to arrange two bearings with a single degree-of-freedom in series (or stacked one on top of the other); this means that the bandwidth in both directions can be the same since inertia and stiffness properties are the same in both directions. The arrangement also eliminates Bryan offsets [4] since the actuation forces are applied through the center-of-stiffness which is located at the geometric center of the bearing. In addition, Abbé offsets are elimi-

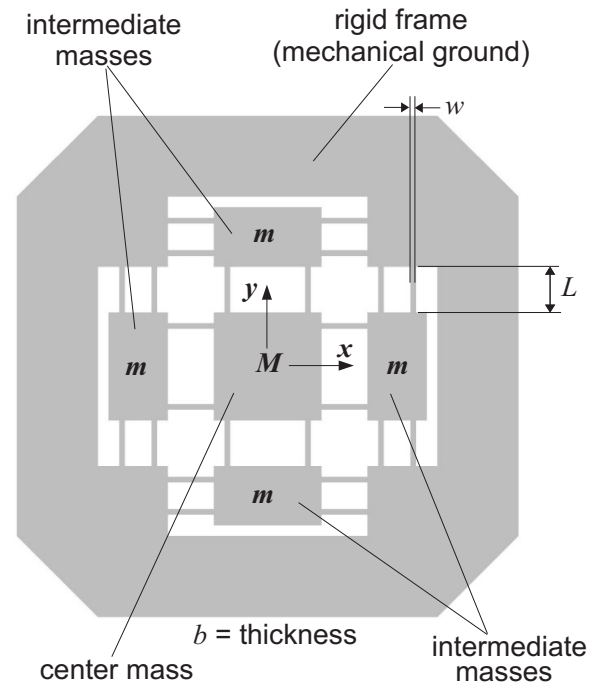


FIGURE 1. Dimensions and lumped parameters of a rectilinear bearing.

nated when the gaging point is also located at the center of the central mass and displacements are measured in-line with the actuation forces; this is the case when the bearing is used in our micro roundness instrument [2, 3]. Finally, the symmetric geometry of the bearing is very beneficial for minimizing the effect of thermal expansion.

It is reasonable to estimate the static stiffness of the rectilinear bearing using simple beam theory. A fixed-guided beam with Young's modulus  $E$  and dimensions of length  $L$ , width  $w$ , and thickness  $b$  bends and produces a displacement at the guided end when subjected to a transverse force. The beam acts as a linear spring with the stiffness  $k_b$  given in Eq. 1.

$$k_b = \frac{Ebw^3}{L^3} \quad (1)$$

An estimate for the stiffness of the bearing in the  $x$  or  $y$  direction is obtained by combining the bending stiffness of twelve beams in parallel. Estimates of  $k_x$  and  $k_y$  are equal and given in Eq. 2.

$$k_x = k_y = 12k_b = \frac{12Ebw^3}{L^3} \quad (2)$$

This simple approach does not consider two important aspects of this bearing, which should not be neglected for precision applications. First, it neglects the deformation that occurs due to compression and tension in the twelve beams that are orthogonal to the applied load. This deformation causes the displacement of the central mass to be slightly different than for the intermediate masses. Second, it cannot consider cross-coupling effects within the rectilinear displacements due to stiffening or softening of the stressed beams. In this paper, we present a simple multi-degree of freedom analytical model to address the first aspect and use finite element analysis (FEA) for the second aspect. Either method can predict the lowest resonant frequency in the rectilinear direction.

### MULTI-DEGREE OF FREEDOM LUMPED SPRING-MASS MODEL

The static stiffness of the bearing, in both the  $x$  and  $y$  directions, is predicted by the lumped spring-mass model shown in Fig. 2. An actuator (typically made of piezoelectric material) elongates by a quantity  $u_p$ . Due to the axial compliance  $k_a$  of the beams, given in Eq. 3, the displacements of the central mass  $u_c$ , actuation mass  $u_a$ , and measuring mass  $u_m$  all differ. Furthermore, the displacement of the actuation mass will be less than the elongation of the actuator due to the stiffness of the actuator  $k_p$ . With this model, it is possible to estimate the measuring error  $e_m$  and the lost motion  $e_l$  using Eqs. 4 and 5.

$$k_a = \frac{Ebw}{L} \quad (3)$$

$$e_m = u_c - u_m \quad (4)$$

$$e_l = u_p - u_c \quad (5)$$

The stiffness of the springs for this model are determined by combining either the bending stiffness  $k_b$  or the axial stiffness  $k_a$  of the fixed-guided beams in parallel. The two intermediate masses along the direction of the load are joined to mechanical ground with springs of stiffness  $4k_b$ . The

pair of the two lateral intermediate masses is connected to ground with a spring of stiffness  $8k_a$ . The center mass is joined to the two longitudinal intermediate masses with two springs of stiffness  $2k_a$  and to the lateral intermediate masses with a spring of stiffness  $4k_b$ .

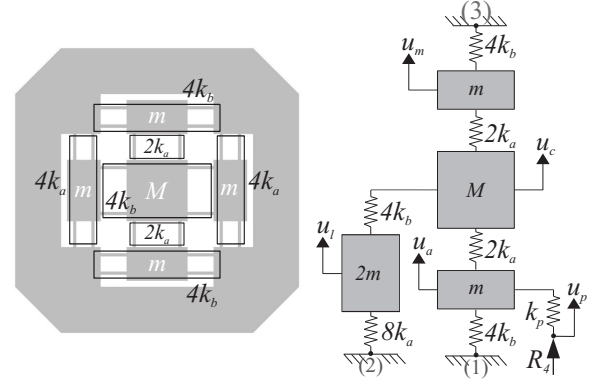


FIGURE 2. Stiffness model incorporating axial and bending stiffness for displacements in one direction.

Static equilibrium at each node of the spring-mass model provides a linear system of equations that are expressed in matrix form by Eq. 6. In Eq. 7, the unknown displacements are grouped into a vector of nodal displacements  $\mathbf{U}$ , and the loads applied to each node are grouped into  $\mathbf{F}$  in Eq. 8.

$$[\mathbf{K}]\mathbf{U} = \mathbf{F} \quad (6)$$

$$\mathbf{U} = [u_a \quad u_l \quad u_c \quad u_m]^T \quad (7)$$

$$\mathbf{F} = [k_p u_p \quad 0 \quad 0 \quad 0]^T \quad (8)$$

The stiffness matrix  $[\mathbf{K}]$  is given in Eq. 9 with some of the terms depending upon  $k'$  given in Eq. 10.

$$[\mathbf{K}] = \begin{bmatrix} -(k' + k_p) & 0 & 2k_a & 0 \\ 0 & -(4k_b + 8k_a) & 4k_b & 0 \\ 2k_a & 4k_a & -k' & 2k_a \\ 0 & 0 & 2k_a & -k' \end{bmatrix} \quad (9)$$

$$k' = 4k_b + 2k_a \quad (10)$$

Solving the linear system of equations in Eq. 6 gives the displacements in  $\mathbf{U}$ . The reaction forces at the three connections to ground  $R_1$ ,  $R_2$ , and  $R_3$  and the reaction  $R_4$  at the node where  $u_p$  is displaced are given by Eq. 11.

$$\begin{bmatrix} R_1 \\ R_2 \\ R_3 \\ R_4 \end{bmatrix} = \begin{bmatrix} -k_1 & 0 & 0 & 0 \\ 0 & -4k_2 & 0 & 0 \\ 0 & 0 & -k_1 & 0 \\ -k_p & 0 & 0 & k_p \end{bmatrix} \begin{bmatrix} u_a \\ u_l \\ u_m \\ u_p \end{bmatrix} \quad (11)$$

The same spring-mass model can be used to predict the lowest resonant frequency from an undamped modal analysis of the bearing. The free vibration of the bearing is formulated as shown in Eq. 12, where the stiffness matrix  $[\mathbf{K}]$  is given by Eq. 9, the mass matrix  $[\mathbf{M}]$  is given in Eq. 13, and  $\mathbf{U}$  is the displacement vector.

$$[\mathbf{M}]\ddot{\mathbf{U}} + [\mathbf{K}]\mathbf{U} = \mathbf{0} \quad (12)$$

$$[\mathbf{M}] \equiv \begin{bmatrix} m & 0 & 0 & 0 \\ 0 & 2m & 0 & 0 \\ 0 & 0 & M & 0 \\ 0 & 0 & 0 & m \end{bmatrix} \quad (13)$$

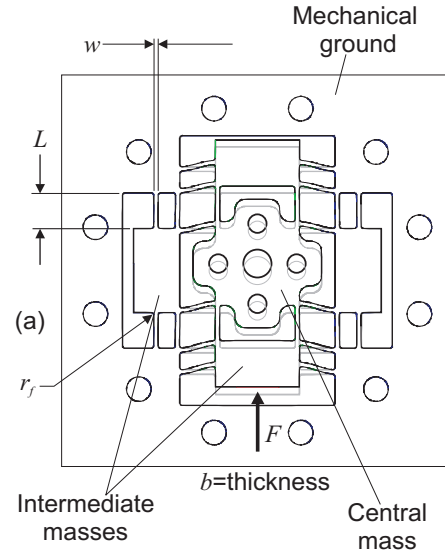
Assuming harmonic motion at each node yields the eigenvalue problem in Eq. 14, whose solution gives four resonant frequencies  $\omega_i$  and mode shapes  $\mathbf{U}_i$ . The lowest resonant frequency and its corresponding mode shape are associated with vibration in the direction of displacement and will therefore limit the bandwidth of a servo-controlled positioning system.

$$[\mathbf{M}]^{-1}[\mathbf{K}]\mathbf{U} = \omega^2\mathbf{U} \quad (14)$$

#### APPLICATION IN MICRO METROLOGY

The rectilinear bearing is ideal for metrology applications. It is essentially frictionless, so the displacement is directly proportional to the applied force. The resolution of the output displacement is then directly related to the resolution of the input force; using piezo-actuators for generating this force can achieve subnanometer positioning resolution. Therefore, we are using two of these elastic bearings, shown in Fig. 3, in the design of a new instrument that measures the roundness of micro components [2].

The first bearing is mounted on the top of an air bearing spindle (Professional Instruments, Model 4R) that rotates the measured sample. The bearing centers the sample's centerline on the spindle's axis-of-rotation within a few nanometers. The resonant frequencies far exceed 1 kHz, which is recommended for scanning probe microscopy [5]. Translation in two orthogonal directions result when two piezoelectric stack actuators (Piezomechanick) press against the actuated intermediate masses. The motions of the opposite intermediate masses are measured by two non-contact capacitive displacement sensors with 0.4 nm resolution (Lion Precision). The second rectilinear bearing moves a probe tip in two



Design Parameters:  $b = 25.16$  mm,  $L = 8.13$ mm,  $w = 0.95$  mm,  $r_j = 0.64$  mm

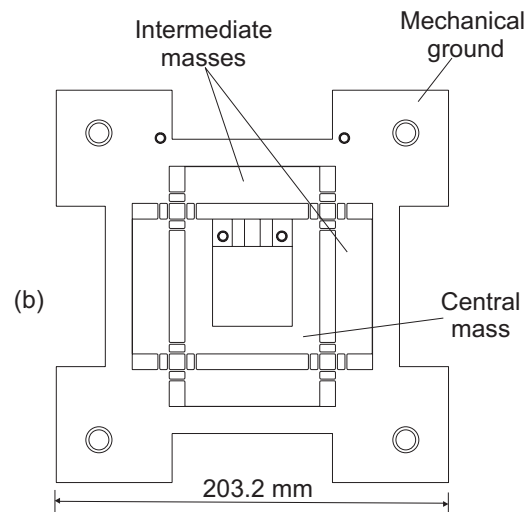


FIGURE 3. Rectilinear elastic bearings used in the micro-roundness instruments: (a) Bearing for centering sample on axis-of-rotation and (b) Bearing for positioning probe tip.

orthogonal directions, also with piezoelectric actuators and capacitive displacement sensing. A major drawback of an elastic bearing is its limited range of displacement. This is not an issue for this metrology equipment, because the fine resolution required for measuring the roundness of micro-shafts stays within the travel range of the bearing ( $\pm 10$   $\mu\text{m}$ ).

Even though the external dimensions of the two bearings are different, they are designed to present the same stiffness. The beams in both

bearings have the same dimensions  $L$ ,  $w$ , and  $b$ . However their resonant frequencies are different, because their intermediate masses  $m$  and the center masses  $M$  are not equal due to the dimensional differences.

Two prototype bearings were manufactured at Professional Instruments. Their static stiffnesses and resonant frequencies were measured experimentally by Loychik [6], and their values are compared with the results of lumped spring-mass model and additional finite element analyses described in the following section.

### FINITE ELEMENT ANALYSES

The analytical results for the stiffnesses and lowest resonant frequency for the two bearings used in the micro roundness instrument are validated with a finite element model. FEA is also used to further investigate possible cross-coupling effects that result from stress stiffening or softening. Although the lumped spring-mass model is limited to one direction, the FEA can apply simultaneous loads in both orthogonal directions and give other mode shapes. In addition, we now include fillets with radius  $r_f$  at the ends of the beams, which were not included in the lumped spring-mass model.

#### Static stiffness

The first result that can be verified by FEA is the static stiffness of the bearing. Only one load is applied on the bearing, and the FEA program returns the resulting displacement in the direction of the load. The stiffness of the bearing is simply defined as the ratio of the load to the displacement. The analytical, FEA and experimental results are listed in Table 1, and there is less than 1.5% of variation between the results.

TABLE 1. Comparison of the analytical, FEA and experimental results of the static analysis.

	Ana.	FEA	Exp.
Bearing stiffness (N/ $\mu$ m)	93.7	94.4	95.0

#### Undamped modal analysis

The modal analysis performed by FEA yields more modes than the lumped spring-mass model and the experiment, since FEA considers displacements in more than one direction. The analytical model determines the displacements oc-

curing in the direction of the load, but a displacement in any other direction is omitted. Similarly, the experiment was run by placing a capacitance probe along the direction of the load, so the experimental results exclusively correspond to the displacement in this direction, and any motion in other directions were not collected.

As shown in Fig. 4(a), the first mode corresponds to a displacement in the direction of the load, which would correspond with the sensitive direction in most applications. The second mode, which occurs at the same frequency, is simply a symmetric mode. Table 2 lists the resonant frequencies determined for the first mode shape by the analytical model, FEA model, and the experiments conducted by Loychik [6]. There is some discrepancy with the experimental result, which we cannot explain at this time. The frequencies given by FEA are 2% to 11% greater than the values calculated with the analytical model. This is probably due to the addition of the fillet radius in the FEA model, which stiffens the beams and increases the resonant frequencies.

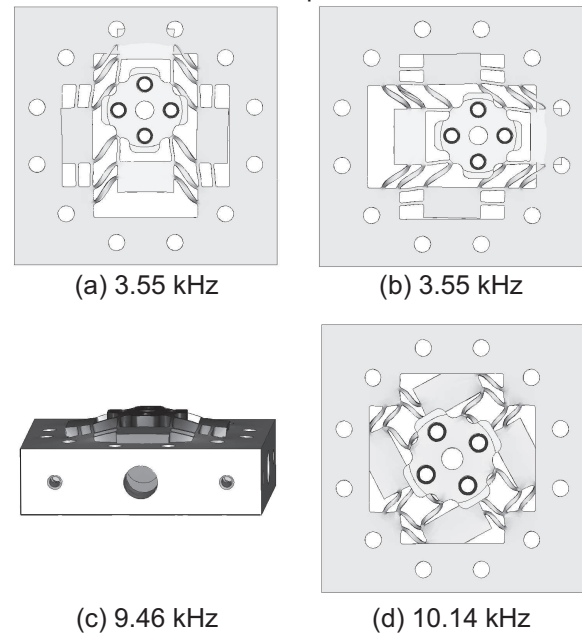


FIGURE 4. Four first mode shapes of the bearing for centering sample on axis-of-rotation. (a) Linear displacement in the load direction, (b) Linear displacement normal to the load direction, (c) Translation out of the plane and (d) Rotation of the center mass.

The third and fourth modes shown in Fig. 4(c) and 4(d), which have significantly higher reso-

TABLE 2. Comparison of the analytical, FEA and experimental results of the modes in one direction.

	Ana.	FEA	Exp.
Bearing (a), 1 <sup>st</sup> mode (kHz)	3.47	3.55	4.10
Bearing (b), 1 <sup>st</sup> mode (kHz)	1.42	1.60	1.62

nant frequencies, are less critical. They do not correspond with displacements in the sensitive directions, and they do not critically affect the bandwidth of servo-controlled systems. The third mode is motion out of the plane of the bearing, and the fourth mode tends to rotate the central mass about its center. The lumped spring-mass model is not capable of predicting either of these two modes.

### Cross-coupling effects

As seen in the previous sections, beams that are parallel to the displacement are loaded axially, and some are loaded in tension while others are loaded in compression. Axial tensile stress within a beam increases its bending stiffness (stiffens), and compressive stress decreases its bending stiffness (softens). This causes cross-coupling between simultaneous displacements in the  $x$  and  $y$  directions. The analytical model does not predict this effect because it only deals with loads in one direction. So to investigate this phenomena, we employ another finite element analysis using simultaneous forces applied in both the  $x$  and  $y$  directions and investigate changes in the stiffness of the bearing.

The analysis of the cross-coupling effect is a three-step procedure, as illustrated in Fig. 5. First, a preload force  $F_y$  is applied in the  $y$ -direction; the beams that are parallel to the  $x$ -axis are bent, and the beams parallel to the  $y$ -axis are either compressed or extended. The second step consists of applying a load  $F_x$  in the  $x$ -direction, which also causes bending and compression/elongation. Then the third step increments the load in the  $x$ -direction by one unit ( $F_x + 1$ ); this step is required to take into consideration the change of geometry of the bearing subject to loads. The solutions are performed using large-displacement and stress-stiffening options. The stiffness in the  $x$  direction under the simultaneous loads  $F_x$  and  $F_y$  is computed using the displacement of the central mass that occurs in

the  $x$ -direction between steps two and three using Eq. 15.

$$k_x = \frac{1}{u_x(3) - u_x(2)} \quad (15)$$

The results of the cross-coupling effects analysis for the bearing locating the sample are displayed in Fig. 6. Application of the preload force  $F_y$  reduces the stiffness of the bearing in the  $x$ -direction  $k_x$ . A preload of 1000 N lowers the stiffness by 3.5%. This softening effect can therefore introduce detectable positioning errors that should be taken into account in high-precision applications requiring nanometer-level accuracy.

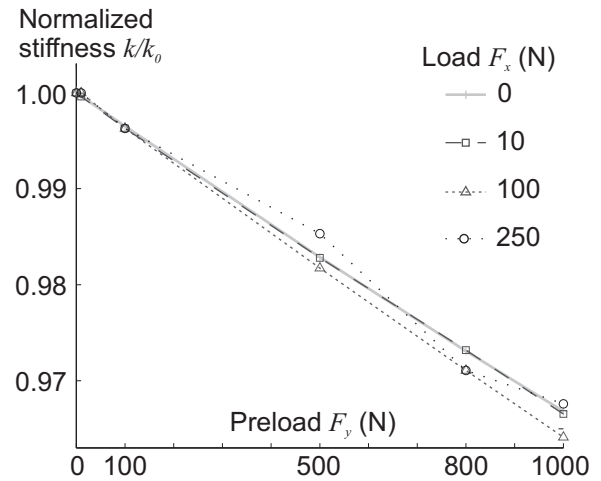


FIGURE 6. Normalized stiffness  $k/k_0$  as a function of preload  $F_y$ . Load  $F_x$  is kept constant for each curve. The reference stiffness  $k_0$  is found when no load and no preload or applied, i.e.  $k_0 = 94.4 \text{ N}/\mu\text{m}$ .

### CONCLUSIONS

A lumped spring-mass model of a rectilinear flexural bearing has been developed for static and modal analyses in one direction. The exactness of the model has been confirmed by FEA and experimental studies of two prototyped bearings from a metrology instrument measuring the roundness of micro components. Moreover cross-coupling effects of two combined orthogonal loads have been demonstrated by FEA. These effects alter the stiffness of an elastic bearing and hence its accuracy. Quantifying them is important when predicting the accuracy of an instrument based on elastic bearings.

### ACKNOWLEDGEMENTS

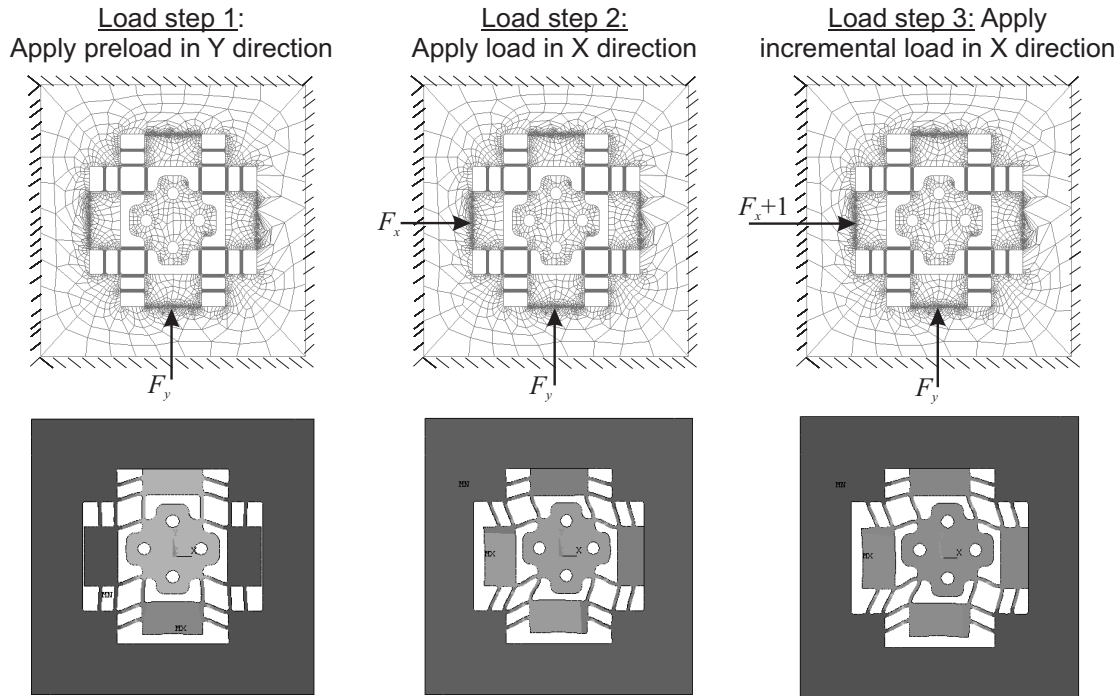


FIGURE 5. Procedure for simulating the cross-coupling effect on FEA. (1) First, apply a preload in one direction. (2) Then apply the nominal load in a direction normal to the preload. (3) Finally, increment the load.

The authors acknowledge Mr. Neil Loychik for initially designing the bearings used in the micro roundness instrument [6], and we also acknowledge Professional Instruments Co. ([www.airbearings.com](http://www.airbearings.com)), especially Dave Arneson, for assisting with the manufacture of the bearings.

## REFERENCES

- [1] A.E. Holman, C.D. Laman, P.M.L.O. Scholte, W.C. Heerens, and F. Tuijstra. A calibrated scanning tunneling microscope equipped with capacitive sensors. *Review of Scientific Instruments*, 67:2274–2280, 1996.
- [2] N. Loychik, M. Barraja, A. Khan, R.R. Vallance, E. Marsh, and D. Arneson. Mechanical design of a precision instrument for measuring the roundness profiles of micro shafts. In *Proceedings of ASME 2006 International Conference on Manufacturing Science & Engineering*, 2006.
- [3] M. Barraja, R.R. Vallance, N. Loychik, E.R. Marsh, and D. Arneson. Design and evaluation of a prototype instrument for measuring roundness profiles of micro-shafts. In *Proceedings of the 21st ASPE Annual Meeting*, 2006.
- [4] J. B. Bryan. The Abbé principle revisited: an updated interpretation. *Precision Engineering*, 1(3):129–132, July 1979.
- [5] D.W. Pohl. Some design criteria in scanning tunneling microscopy. *IBM J. Res. Develop.*, 30(4):417–427, July 1986.
- [6] N. Loychik. Design of a prototype scanning probe instrument for the metrology of microshafts. Master's thesis, The George Washington University, 2007.